

Nuclear symmetry energy at work in heavy ion reactions: new results from the INDRA-FAZIA apparatus

C Ciampi^{*1,2}, S Piantelli², G Casini², G Pasquali^{1,2}, L Baldesi^{1,2},
 S Barlini^{1,2}, B Borderie³, R Bougault⁴, A Camaiani⁵, A Chbihi⁶,
 D Dell'Aquila^{7,8}, M Cicerchia⁹, J A Dueñas¹⁰, Q Fable¹¹, D Fabris¹²,
 J D Frankland⁶, C Frosin^{1,2}, T Génard⁶, F Gramegna⁹, D Gruyer⁴,
 M Henri⁶, B Hong^{13,14}, S Kim¹⁵, A Kordyasz¹⁶, T Kozik¹⁷,
 M J Kweon^{13,18}, J Lemarié⁶, N Le Neindre⁴, I Lombardo¹⁹, O Lopez⁴,
 T Marchi⁹, S H Nam^{13,14}, A Ordine²⁰, P Ottanelli², J Park^{13,14},
 J H Park^{13,18}, M Pârligă^{4,21}, G Poggi^{1,2}, J Quicray⁴,
 A Rebillard-Soulié⁴, A A Stefanini^{1,2}, S Upadhyaya¹⁷, S Valdré²,
 G Verde^{11,19}, E Vient⁴ and M Vigilante^{20,22}
(INDRA-FAZIA collaboration)

¹Dipartimento di Fisica e Astronomia, Università di Firenze, 50019 Sesto Fiorentino, Italy

²INFN - Sezione di Firenze, 50019 Sesto Fiorentino, Italy

³Université Paris-Saclay, CNRS/IN2P3, IJCLab, 91405 Orsay, France

⁴Normandie University, ENSICAEN, UNICAEN, CNRS/IN2P3, LPC Caen, F-14000 Caen, France

⁵KU Leuven, Instituut voor Kern- en Stralingsphysica, 3001 Leuven, Belgium

⁶Grand Accélérateur National d'Ions Lourds (GANIL), CEA/DRF-CNRS/IN2P3, Boulevard Henri Becquerel, F-14076 Caen, France

⁷Dipartimento di Chimica e Farmacia, Università degli Studi di Sassari, 07100 Sassari, Italy

⁸INFN - Laboratori Nazionali del Sud, 95123 Catania, Italy

⁹INFN - Laboratori Nazionali di Legnaro, 35020 Legnaro, Italy

¹⁰Departamento de Ingeniería Eléctrica y Centro de Estudios Avanzados en Física, Matemáticas y Computación, Universidad de Huelva, 21007 Huelva, Spain

¹¹Laboratoire des 2 Infinis - Toulouse (L2IT-IN2P3), Université de Toulouse, CNRS, UPS, F-31062 Toulouse Cedex 9, France

¹²INFN - Sezione di Padova, 35131 Padova, Italy

¹³Center for Extreme Nuclear Matters (CENuM), Korea University, Seoul 02841, Republic of Korea

¹⁴Department of Physics, Korea University, Seoul 02841, Republic of Korea

¹⁵Institute for Basic Science, Daejeon 34126, Republic of Korea

¹⁶Heavy Ion Laboratory, University of Warsaw, 02-093 Warszawa, Poland

¹⁷Marian Smoluchowski Institute of Physics, Jagiellonian University, 30-348 Krakow, Poland

¹⁸Department of Physics, Inha University, Incheon 22212, Republic of Korea

¹⁹INFN - Sezione di Catania, 95123 Catania, Italy

²⁰INFN - Sezione di Napoli, 80126 Napoli, Italy

²¹"Horia Hulubei" National Institute for R&D in Physics and Nuclear Engineering (IFIN-HH), P. O. Box MG-6, Bucharest Magurele, Romania

²²Dipartimento di Fisica, Università di Napoli, 80126 Napoli, Italy

E-mail: ciampi@fi.infn.it



Content from this work may be used under the terms of the [Creative Commons Attribution 3.0 licence](#). Any further distribution of this work must maintain attribution to the author(s) and the title of the work, journal citation and DOI.

Abstract. The recently coupled INDRA-FAZIA apparatus offers unique opportunities to investigate heavy ion collisions at Fermi energies by combining the optimal identification capabilities of FAZIA and the large angular coverage of INDRA. We present a selection of the results of the analysis of the first experimental campaign performed with INDRA-FAZIA, in which the four reactions $^{58,64}\text{Ni} + ^{58,64}\text{Ni}$ have been studied at two different beam energies (32 and 52 MeV/nucleon) in the intermediate energy regime. The present work is focused on the isospin diffusion effects in semiperipheral and peripheral collisions. A stronger isospin equilibration is found at 32 MeV/nucleon than at 52 MeV/nucleon, as expected due to a shorter projectile-target interaction time in the latter case.

1. Introduction

The Nuclear Equation of State (NEoS), describing the behavior of nuclear matter as a function of thermodynamic variables, has been a widely investigated topic since many years. More specifically, many efforts are being made in order to constrain the values of the parameters defining the nuclear density dependence of the symmetry energy term of the NEoS. The interest in this topic is manifold, ranging from astrophysics (for the description of neutron stars) to nuclear physics. Heavy ion collisions in the intermediate energy regime (20 – 100 MeV/nucleon) provide a tool to study the properties of nuclei far from equilibrium conditions of temperature and density, in view of extrapolating the information to infinite nuclear matter [1]. Among other topics, they allow to investigate the isospin transport phenomena (drift and diffusion) [2], i.e. the nucleon exchange processes between projectile and target taking place during the dynamical phase of the reaction. The *isospin diffusion* is driven by the presence of an isospin gradient and induces the isospin equilibration of the system, the *isospin drift* takes place whenever a density gradient is present and is responsible for the neutron enrichment of low density regions. These processes are governed by the symmetry energy of the NEoS and could therefore provide constraints on its parametrization.

2. The INDRA- FAZIA experimental apparatus

The investigation of such phenomena requires a very good isotopic identification capability in a wide range of charge number Z and energy of the reaction products, as that provided by the recently coupled INDRA-FAZIA apparatus, located in GANIL (Caen, France). The setup exploits the optimal mass identification performance of FAZIA [3, 4] for the isotopic discrimination of quasiprojectile-like fragments (QP), together with the large angular coverage provided by INDRA [5]. Both these telescope arrays, that have been developed separately, are optimized for the detection and identification of the ejectiles produced in heavy ion collisions at Fermi energies. In order to couple the two setups, the first 5 INDRA rings have been removed and replaced by 12 FAZIA blocks, covering the most forward polar angles where the heaviest fragments belonging to the QP phase space are mostly focused; more details on the apparatus are given in Ref. [6]. The first INDRA-FAZIA experiment [6] has been carried out in 2019, right after the coupling of the two detection arrays: here, all the four possible combinations of the two reaction partners ^{58}Ni and ^{64}Ni have been studied, in order to compare the results obtained for the two asymmetric systems with those of the two symmetric ones. The four reactions have been investigated at two different incident beam energies, 32 and 52 MeV/nucleon.

3. Data analysis

We present a selection of the first results of the analysis of the experimental data described above, focusing on the outcome of semiperipheral and peripheral collisions for which a generally binary exit channel is expected, with the production of a QP and a quasitarget (QT) together with lighter emissions.

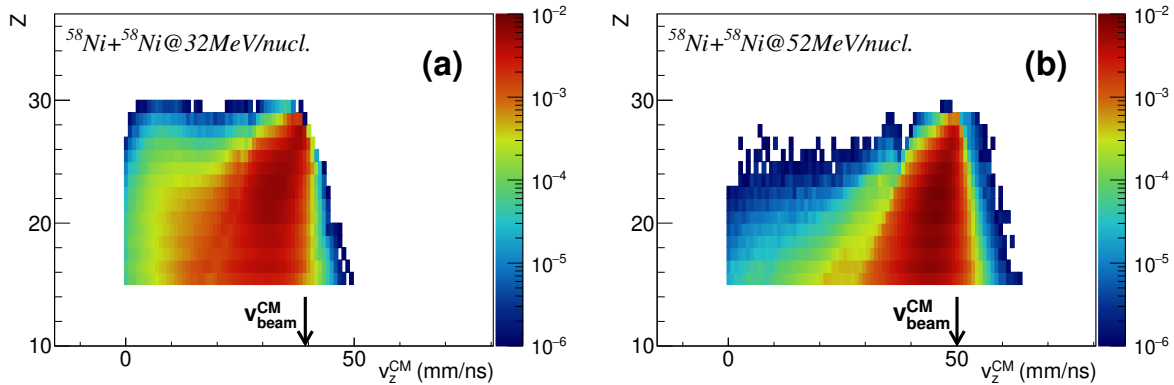


Figure 1. Experimental charge Z vs velocity v_z^{CM} correlations for the QP remnant of the events falling in the QP evaporation channel selection, obtained for the reaction $^{58}\text{Ni} + ^{58}\text{Ni}$ at 32 MeV/nucleon (a) and 52 MeV/nucleon (b). Similar results are obtained for the other reactions. The plots are normalized to their integral.

In order to select the QP evaporation channel we require the presence of a single heavy fragment (the QT being below the detection threshold of the setup), with $Z \geq 15$, forward directed in the CM reference frame, accompanied only by light charged particles (LCPs, $Z = 1, 2$) or intermediate mass fragments (IMFs, $Z = 3, 4$) [6]. Figure 1 shows the correlation between the charge Z and the component along the beam axis of the CM velocity v_z^{CM} of the biggest fragment (identified as QP remnant) in the events thus selected, obtained for a sample reaction at 32 MeV/nucleon (a) and 52 MeV/nucleon (b). In both plots, a strongly populated area is evident, extending towards the original projectile charge $Z_{proj} = 28$ and velocity (v_{beam}^{CM} , indicated with a black arrow on each plot): these characteristics are therefore compatible with those of a QP remnant. The correlation in Fig. 1(a) for the reaction at the lower bombarding energy also shows the presence of some heavy fragments in the $v_z^{CM} \approx 0$ mm/ns region, compatible with the outcome of more central events resulting in an incomplete fusion process. These are not present at 52 MeV/nucleon due to the more multifragmentation-like character of central collisions, as expected for a higher beam energy. However, these central events will not be considered in the isospin analysis presented in the following, thanks to the cuts that will be imposed on the reaction centrality. Similar observations can be done on the correlations obtained for the other three reactions. The experimental charge and velocity distributions for the QP remnant have also been compared to the predictions of simulations with the dynamical transport model AMD (antisymmetrized molecular dynamics [7]) coupled to GEMINI++ [8] as afterburner, filtered according to the apparatus acceptance, generally showing a good agreement [6].

In view of studying the evolution of the isospin equilibration effect with the reaction centrality, we select the reduced QP remnant momentum as order parameter [9], defined as $p_{red} = (p_z^{QP}/p_{beam})_{CM}$, where p_z^{QP} is the beam axis component of the QP remnant momentum and p_{beam} is the original projectile momentum, both in the CM reference frame. The AMD+GEMINI++ simulations have been exploited to test the correlation of this centrality estimator with the reduced impact parameter $b_{red} = b/b_{gr}$ (b_{gr} being the grazing impact parameter): the results are reported in Fig. 2 for a sample reaction at 32 MeV/nucleon (a) and 52 MeV/nucleon (b). A clear correlation is visible at both energies, well defined for p_{red} values down to ~ 0.4 : the p_{red} variable can be therefore considered reliable to study semiperipheral and peripheral collisions. Similar b_{red} vs p_{red} correlations are obtained for the other reactions. More specifically, in Ref. [6] we have shown by superimposing the plots of the average b_{red} as a function of p_{red} that the behavior of the correlation is only slightly dependent on the beam

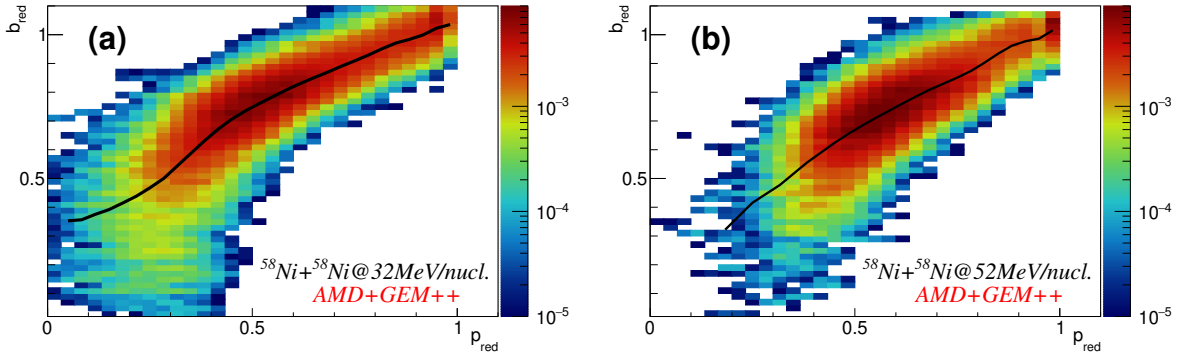


Figure 2. AMD+GEMINI++ prediction of the correlation between b_{red} and p_{red} for the events in the QP evaporation channel for the reaction $^{58}\text{Ni} + ^{58}\text{Ni}$ at 32 MeV/nucleon (a) and 52 MeV/nucleon (b). Similar results are obtained for the other reactions. The plots are normalized to their integral. The average b_{red} for each p_{red} bin is indicated with a black line.

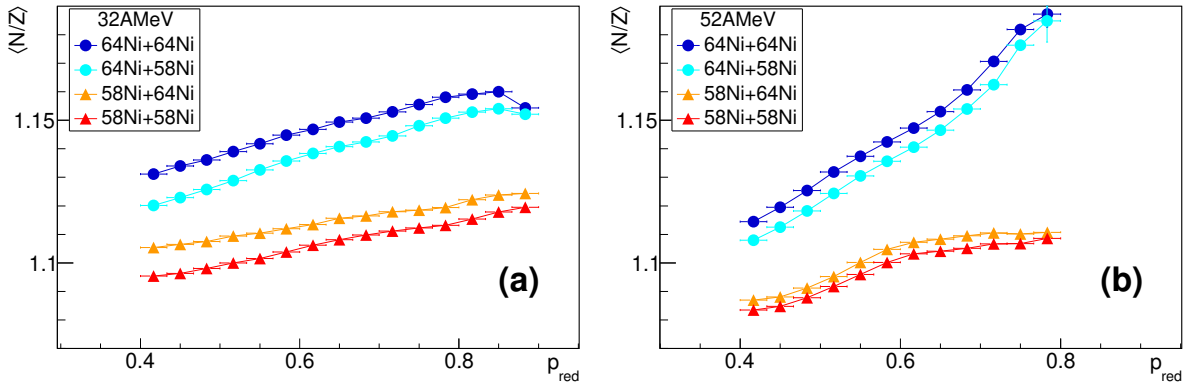


Figure 3. Experimental average neutron-to-proton ratio $\langle N/Z \rangle$ of the QP residue as a function of p_{red} for the four reactions at 32 MeV/nucleon (a) and 52 MeV/nucleon (b). Vertical error bars represent statistical errors, while horizontal error bars are equal to the p_{red} bin width.

energy and almost independent of the system.

Taking advantage of the optimal isotopic identification provided by FAZIA for the QP phase space, we exploit the average neutron-to-proton ratio $\langle N/Z \rangle$ of the QP remnant as isospin related observable. Figure 3 shows the $\langle N/Z \rangle$ of the QP remnant as a function of p_{red} for the four reactions at 32 MeV/nucleon (a) and 52 MeV/nucleon (b). In both plots, a clear hierarchy of the four reactions is present, with the $\langle N/Z \rangle$ of the asymmetric systems always between those of the symmetric systems: the gap between the $\langle N/Z \rangle$ obtained for the asymmetric and symmetric reactions sharing the same projectile (same marker shape in Fig. 3) reveals a dependence of the isospin content of the QP remnant on the isospin of the target of the reaction, and represents an evidence of the dynamical effect of isospin diffusion surviving the action of statistical evaporation. This gap also tends to increase for decreasing p_{red} , i.e., for less peripheral collisions.

The isospin equilibration can be further highlighted by exploiting the isospin transport ratio technique, first introduced in Ref. [10] and defined as:

$$R(X_i) = \frac{2X_i - X_{AA} - X_{BB}}{X_{AA} - X_{BB}} \quad (1)$$

where X is an isospin sensitive observable, such as the $\langle N/Z \rangle$ of the QP residue, A and B are

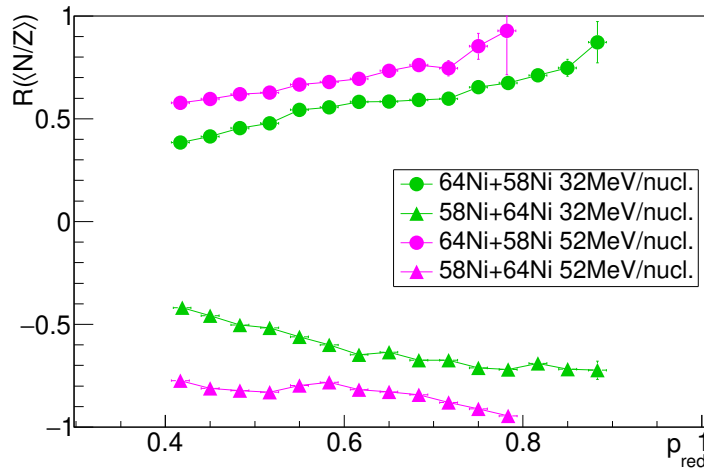


Figure 4. Experimental isospin transport ratio calculated exploiting the $\langle N/Z \rangle$ of the QP residue as a function of p_{red} shown in Fig. 3. The results for the asymmetric reactions at 32 MeV/nucleon (52 MeV/nucleon) are plotted in green (magenta). Statistical errors are plotted on the y -axis.

the two nuclear species employed in the reactions (A being the more neutron rich one), and i is one of their four possible combinations. By definition, if the ratio is calculated for the symmetric reactions a value of $+1$ (-1) is obtained for the neutron rich (deficient) one. For the asymmetric reactions, the limit of the non-equilibrated condition corresponds to $R(X_i) = \pm 1$, while for a fully isospin equilibrated outcome $R(X_{AB}) = R(X_{BA})$. The isospin transport ratio can evidence the effect of equilibration in an asymmetric system by taking the information on the corresponding neutron rich and neutron deficient symmetric reactions as a reference, thus largely bypassing most of the effects acting similarly on the four systems (e.g. statistical de-excitation [11]). In Fig. 4 the isospin transport ratios obtained for the two asymmetric systems $^{64}\text{Ni}+^{58}\text{Ni}$ and $^{58}\text{Ni}+^{64}\text{Ni}$ are plotted as a function of p_{red} , using different marker shapes depending on the projectile of the reaction as in Fig. 3. The results at 32 MeV/nucleon (52 MeV/nucleon) are plotted in green (magenta). At both energies, more peripheral collisions correspond to $R(\langle N/Z \rangle_{AB,BA})$ values closer to ± 1 , while for decreasing p_{red} (i.e., increasing centrality) the two “branches” of the ratio tend towards each other, indicating the equilibrating effect of isospin diffusion. By comparing the results for the two beam energies, it can be noticed that a different degree of isospin equilibration seems to be achieved: indeed, the plots of $R(\langle N/Z \rangle_{AB,BA})$ are closer to each other for the reactions at 32 MeV/nucleon than for those at 52 MeV/nucleon. This difference can be explained, for instance, with a longer interaction time between projectile and target at the lower bombarding energy. These results and observations are based only on experimental data and are therefore model independent. However, in Ref. [6] we have also taken into account the slightly different p_{red} vs b_{red} correlation found for the two beam energies according to AMD+GEMINI++, by reporting the isospin transport ratio as a function of b_{red} , and the different degree of isospin equilibration in the two cases is still evident.

4. Conclusions

In this work the first experiment carried out exploiting the recently coupled INDRA-FAZIA apparatus has been analyzed. The reactions $^{58,64}\text{Ni}+^{58,64}\text{Ni}$ have been investigated for two different bombarding energies, 32 and 52 MeV/nucleon, both belonging to the Fermi energy regime. We have presented a selection of the results concerning the evidence of isospin diffusion effects taking place in the two asymmetric reactions of the dataset, focusing on semiperipheral

and peripheral collisions. An exclusive analysis of the binary exit channel, with the produced QP undergoing statistical de-excitation, has been set by exploiting the selection power provided by the experimental setup. The information on the isospin content of the QP remnants isotopically identified by FAZIA has been used to highlight the isospin diffusion between asymmetric projectile and target. A clear evolution of the phenomenon with the reaction centrality (studied using the reduced QP momentum along the beam axis p_{red} as centrality related parameter) has been found, with a stronger equilibration for more central collisions. By exploiting the isospin transport ratio technique, we have also been able to compare the results obtained for the two beam energies, observing a higher degree of isospin equilibration for the reactions at 32 MeV/nucleon. The latter finding can be explained by a longer projectile-target interaction time at the lower beam energy.

The result presented here is part of a more extensive analysis that takes advantage of the rich information provided by the INDRA-FAZIA apparatus [6]. In an upcoming paper [12] we are extending the analysis presented here to an additional, less-populated output channel, namely the *breakup* or *dynamical fission* of the QP: this latter is a fission process taking place in shorter time scales with respect to statistical fission, and characterised by an anisotropic emission pattern of the two products in case of mass-asymmetric splits, with the lighter fragment generally emitted towards the CM [9, 13–15]. By studying the isospin content of the fissioning QP, “reconstructed” from the two daughter nuclei by considering the sum of their charge and mass numbers and the velocity of their CM, a stronger action of isospin diffusion in the reactions at the lower beam energy is again observed. Further analyses on this dataset, taking into account also other physics phenomena (e.g. those related to the isospin drift [16]), are also foreseen in the near future, together with the forthcoming experiments planned in the scientific program of the INDRA-FAZIA collaboration.

References

- [1] Napolitani P *et al* 2010 *Phys. Rev. C* **81** 044619
- [2] Baran V *et al* 2005 *Phys. Rev. C* **72** 064620
- [3] Bougault R *et al* 2014 *Eur. Phys. J. A* **50** 47
- [4] Valdré S *et al* 2019 *Nucl. Instrum. Methods Phys. Res., Sect. A* **930** 27
- [5] Pouthas J *et al* 1995 *Nucl. Instrum. Methods Phys. Res., Sect. A* **357** 418
- [6] Ciampi C *et al* 2022 *Phys. Rev. C* **106** 024603
- [7] Ono A *et al* 1992 *Prog. Theor. Phys.* **87** 1185
- [8] Charity R J 2010 *Phys. Rev. C* **82** 014610
- [9] Camaiani A *et al* 2021 *Phys. Rev. C* **103** 014605
- [10] Rami F *et al* 2000 *Phys. Rev. Lett.* **84** 1120
- [11] Camaiani A *et al* 2020 *Phys. Rev. C* **102** 044607
- [12] Ciampi C *et al* 2022 *in preparation*
- [13] Casini G *et al* 1993 *Phys. Rev. Lett.* **71** 2567
- [14] Stefanini A A *et al* 1995 *Z. Phys. A* **351** 167
- [15] Piantelli S *et al* 2020 *Phys. Rev. C* **101** 034613
- [16] Piantelli S *et al* 2021 *Phys. Rev. C* **103** 014603